

Rapid synthesis of nanocrystalline SnO₂ by a microwave-assisted combustion method

Lajapathi Chellappan NEHRU^a, Chinnappanadar SANJEEVIRAJA^{b,*}

^aDepartment of Medical Physics, Bharathidasan University, Tiruchirappalli-620 024, India

^bDepartment of Physics, Alagappa Chettiar College of Engineering & Technology, Karaikudi-630 004, India

Received: December 12, 2013; Revised: March 05, 2014; Accepted: March 13, 2014

©The Author(s) 2014. This article is published with open access at Springerlink.com

Abstract: A facile and rapid microwave-assisted combustion method was used to synthesis nanocrystalline SnO₂ powders, through dissolution of tin nitrate (as oxidant) and glycine (as fuel) as starting materials and water as solvent and then heating the resulting solution in a microwave oven. The study suggested that application of microwave heating to produce the nanosize SnO₂ was achieved in a few minutes. The structure and morphology of the as-prepared combustion products were investigated by means of powder X-ray diffraction (PXRD) and scanning electron microscopy (SEM). Fourier transform infrared spectroscopy (FTIR) and Raman spectra confirmed the formation of tetragonal rutile structure SnO₂, and the SEM results indicated the surface characteristic of the products. The as-prepared powders have larger band gap energy as 3.67 eV.

Keywords: nanoparticles; tin oxide; glycine; stoichiometric; combustion; optical

1 Introduction

Semiconducting nanoparticles have been extensively studied from both experimental and theoretical viewpoints because of their potential applications in solar energy conversion, photo catalysis and optoelectronics industry. Nanostructured semiconductors have unusual optical, electronic and chemical properties and wide potential uses as nanoscale devices. The desire for miniaturization is the driving force behind nanoparticle synthesis efforts. Research on the preparation of oxide nanoparticles is an active area being pursued all over the world. Tin oxide (SnO₂) is an important n-type semiconductor

with large band gap and high sensitivity to various toxic or flammable gases, and has been used as one of the promising materials for gas sensors, optoelectronic devices and negative electrodes for lithium batteries [1]. Its ability to transmit visible light or to absorb infrared makes SnO₂ a very attractive material for light conductive films and solar cell coatings [2]. For such applications, nanosize particles are required. Recent research shows that the properties of SnO₂ depend greatly on product's crystallite size and specific surface area [3]. Compared with bulk SnO₂, nanosize SnO₂ has especially good properties and outstanding advantages of low operating temperature and high sensitivity for gas-sensing applications [4].

Many methods have been developed to synthesize SnO₂ nanoparticles, including evaporation of SnO₂ or SnO powders at elevated temperatures [5], solvothermal and hydrothermal routes [6],

* Corresponding author.

E-mail: sanjeeviraja@rediffmail.com

homogeneous precipitation [7], microwave-assisted aqueous solution using a kitchen oven [8] and sol-gel route [9]. Recent papers report on the microwave-assisted hydrothermal synthesis of nanocrystalline SnO₂ and SnO powders [10,11].

Compared to the conventional methods, microwave synthesis has the advantages of producing small and uniform particle size of metal oxides with high purity owing to short reaction time. Microwave-assisted synthesis is a novel method to produce materials, since microwave heating is an *in situ* mode of energy conversion and the microwave heating process is fundamentally different from conventional heating processes. Heat will be generated internally within the material, instead of originating from external sources. By means of this method, many functional materials and compounds with novel structures and properties have been obtained [12].

As for as the literature survey, microwave-assisted combustion synthesis of tin dioxide colloidal suspensions from aqueous solutions of tin nitrate in the presence of glycine is reported for the first time. This method is simple, and the combustion synthesis process is fast, mild, energy-efficient and environmentally friendly to produce SnO₂ nanoparticles using glycine as fuel.

2 Experimental

All the reagents used in the experiments were analytically pure, and were purchased from MERCK Company and used as received without further purification. Nanocrystalline SnO₂ was synthesized by a microwave-assisted combustion synthesis process using glycine as fuel. A schematic representation of the synthesis process used in the current study is graphically shown in Fig. 1. Stoichiometric amounts (based on the thermochemical concepts from propellant chemistry calculation of fuel-to-oxidant mixtures) of tin nitrate and glycine were dissolved in deionized water and poured into a quartz container. Further they were mixed well by magnetic stirring for 1 h, making them almost as homogeneous mixture which was placed in a domestic microwave oven (BPL India Limited, Bangalore, India, Model No. IFB, 17PG1S, microwave 700 W, input range 210–230 V, AC 50 Hz, microwave frequency 2.45 GHz). Initially, the solution boiled and underwent dehydration followed by decomposition with the evolution of large

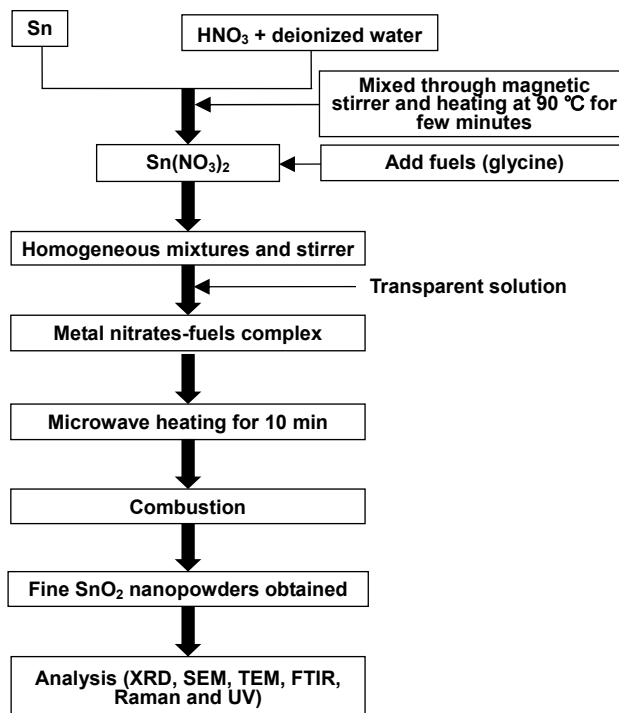


Fig. 1 Schematic representation of the synthesis process.

amount of gases (such as CO₂, H₂O and N₂ formed directly from the reaction between fuel and oxidant) with white fumes coming out from the exhaust opening provided on the top of the microwave oven. After the solution reached the point of spontaneous combustion, it began burning and released lots of heat, vaporized all the solution instantly and became foamy white solid powders.

The synthesized SnO₂ powders' phase formation was identified by powder X-ray diffraction (PXRD) method using X'Pert PRO PANalytical diffractometer with nickel-filtered Cu K α radiation ($\lambda = 0.15418$ nm) as source and operated at 40 kV and 30 mA. The sample was scanned in the 2θ angle ranging from 10° to 80° with minimum step size (0.05°) and minimum scan step time (10.1382 s) mode. The observed peak positions were compared with the standard ICDD data, and Miller indices were assigned to the Bragg peaks. The structure of the as-prepared SnO₂ powders was solved using PXRD method with refinement by Rietveld method. Scanning electron microscopy (SEM) and composition analysis of the sample were obtained using Hitachi S4800 scanning electron microscope equipped with an energy-dispersive X-ray spectrometer (EDX). SEM measurements were mounted on aluminum studs using adhesive graphite

tape and sputter coated with gold before analysis. Infrared spectra were recorded on a Nicolet Avatar 360 FTIR spectrometer using KBr pellets. Raman spectra were taken on a Renishaw model Nicolet FT-Raman 960 Spectrometer (Ar⁺ laser, 480 nm). UV–Vis (ultraviolet–visible) absorption spectra were recorded on a Shimadzu UV-2550 spectrophotometer.

3 Results and discussion

The phase identification of the as-prepared SnO₂ was determined by PXRD. Figure 2 shows the PXRD pattern of the as-prepared SnO₂. It is indicated as the diffraction planes (110), (101), (200), (211), (220), (002), (221), (112), (301), (202) and (321) in the pattern, which can be perfectly indexed to the tetragonal rutile structure. No diffraction peak corresponding to Sn and other impurities is observed in the pattern. The values of lattice parameters ($a = 4.7710 \text{ \AA}$ and $c = 3.2087 \text{ \AA}$) were calculated by the PXRD data, which are in good agreement with the standard diffraction pattern (04-008-8133). Using Scherrer's equation $D = 0.9\lambda / (\beta \cos\theta)$ (where D is the average crystalline size; λ is the wavelength of Cu K α radiation; β is the full width at half maximum (FWHM) of the diffraction peak; and θ is the Bragg's angle), all the half peak widths are very broad, which indicates that the obtained crystallites are small in size, i.e., nanometer size. These results were confirmed by transmission electron microscopy (TEM) observation. The average particle size of SnO₂ is estimated as around 8 nm.

The Rietveld refinement for the investigated SnO₂ is summarized in Table 1. It shows that the refined lattice parameters of stibnite are in good agreement with the reported values. The results of Rietveld analysis demonstrate the tetragonal rutile structure as shown in Fig. 3. In general, R_p (profile factor), R_{wp} (weight

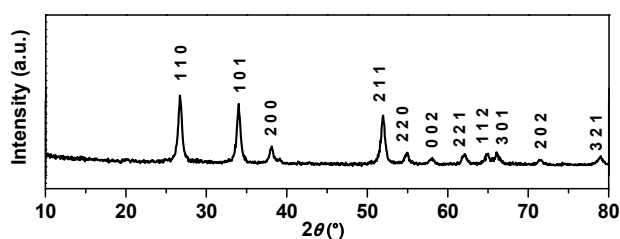


Fig. 2 PXRD patterns of SnO₂ synthesized by a microwave-assisted combustion method.

Table 1 Refined structure parameters of glycine fuel used SnO₂ nanopowders

Space group	$P4_2/mnm$ (136)			
Cell parameters (Rietveld)	a (Å)	4.7907 (2)		
	c (Å)	3.2179 (3)		
	V (Å ³)	73.6784 (3)		
Crystal density (g/cm ³)	5.850			
Atomic positional parameters	x	y	z	B (iso)
Sn (2a)	0	0	0	2.436
O (4f)	0.312	0.312	0	2.631

The structure was refined with the following R factors: R_{exp} (expected weight profile factor, %) = 16.10, R_{wp} (%) = 10.63, R_p (%) = 10.36, R_{Bragg} (Bragg factor, %) = 1.021, DW(Durban–Watson statistic, %) = 0.13 and S (%) = 0.66.

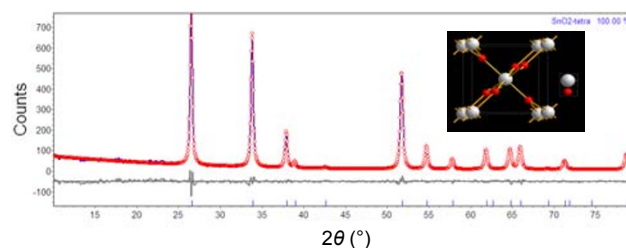


Fig. 3 Observed (blue line), calculated (red line) and difference profiles (black line below) resulting from the adjustment of the de rayos X (DRX) curves of the Rietveld analysis for glycine fuel used SnO₂.

differences between measured and calculated value) and S (good average factor) show decreasing trend with the increase of the weight fraction of albite and suggest that the pattern fitting is accurate. The Rietveld fitting of the SnO₂ phase was performed on the tetragonal rutile structure with space group $P4_2/mnm$ (136). It is formed by a tin atom at the center, surrounded by six oxygen atoms in the vertex. The tin atom is bounded to four oxygen atoms with the same bond length in the basal plane side and to another two apical oxygen atoms with another same bond length. Rietveld refinement is probably the method of choice for determining accurate unit-cell parameters. The refinements of lattice parameters of these phases are $a = 4.7907 \text{ \AA}$, $c = 3.2179 \text{ \AA}$ and $V = 73.6784 \text{ \AA}^3$ for all samples, while the calculated lattice parameters of SnO₂ are slightly higher than the bulk values with respect to the expected ones.

Figure 4(a) shows the SEM micrograph of the as-prepared SnO₂ synthesized by a microwave-assisted combustion process. It can be observed that ultrafine SnO₂ particles with nano sized dimension are interconnected, which shows strong agglomeration accompanied with a lot of small spherically shaped particles. This agglomerate actually consists of much smaller grains of about 10–20 nm in diameter. These morphology results can be attributed to the liberation

of a large amount of gases during a strong combustion reaction, i.e., the rapid release of large volume of gaseous products like H_2O vapor, CO_2 and N_2 , and nitrate ion group acts as an igniter during combustion reaction which promotes the disintegration of the precursor, giving nanocrystalline particles. It is helpful for the finest particle size formation. The agglomerated particles have neck with their neighbors, and they form into spherical shapes intermitted with voids ensuring high surface area. The size can not be exactly determined by the image because they are very small. In spite of that, it is still found from the particle-like morphology. In addition, the EDX analysis (Fig. 4(b)) coupled with SEM confirms that the as-prepared nanocrystalline SnO_2 is composed of tin and oxygen elements, indicating that pure SnO_2 nanoparticles are obtained. The particle size measured by SEM is close to the average particle size obtained from XRD–Rietveld method. The as-synthesized particles are shown in the TEM photograph of nearly tetragonal rutile nanocrystalline SnO_2 particles (Fig. 5). These sizes are well agreed with the Rietveld refinement

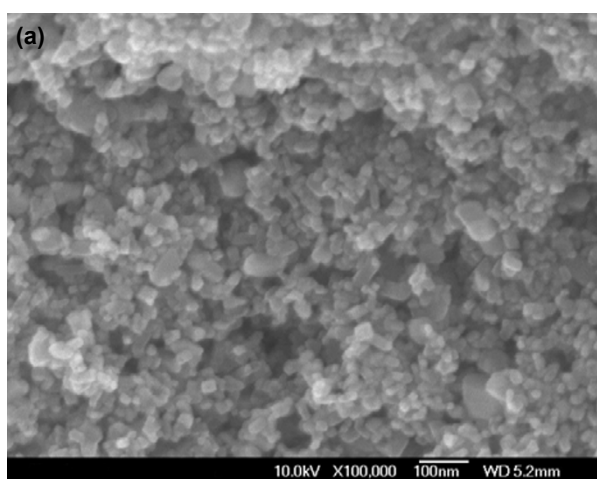


Fig. 4 (a) SEM micrograph and (b) EDX spectrum of SnO_2 powders synthesized by a microwave-assisted combustion method.

method. The corresponding selected area electron diffraction (SAED) image is shown as inset in the TEM image. The diffraction rings clearly confirm that tetragonal structure of SnO_2 has been synthesized successfully. These SnO_2 particle sizes based on XRD and Rietveld refinement results are in quite good agreement with each other and are further confirmed by the particle size estimated by TEM.

The chemical structure of the as-prepared SnO_2 was investigated by FTIR and Raman spectra. Figure 6 shows the FTIR spectrum of the as-prepared nanocrystalline SnO_2 . The absorption bands located in the spectral region of $400\text{--}700\text{ cm}^{-1}$ are caused by different Sn–O or Sn=O stretching modes. The absorption band located around $\sim 460\text{ cm}^{-1}$ has been ascribed to the stretching frequency of oxide group

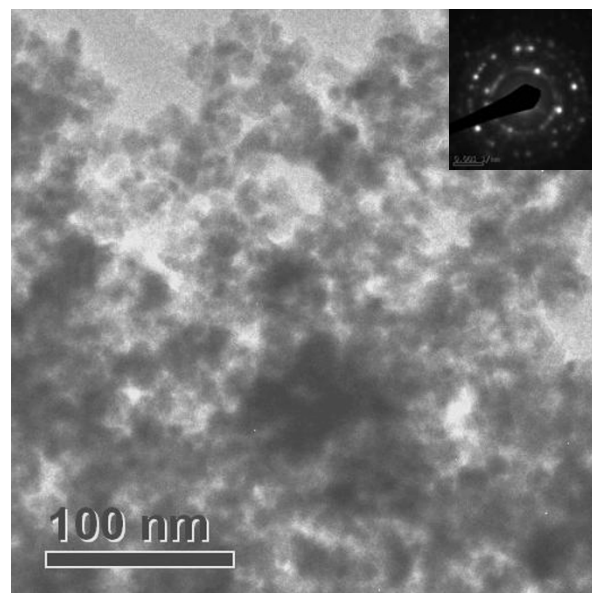


Fig. 5 TEM image of the synthesized SnO_2 nanoparticles.

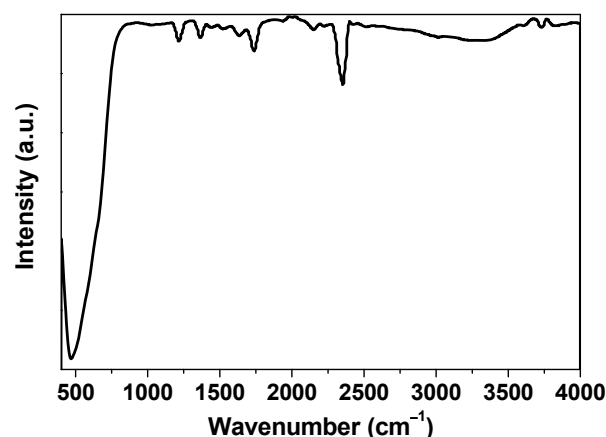


Fig. 6 FTIR spectrum of SnO_2 powders.

(ν_{SnO}). The peaks observed at $\sim 1219 \text{ cm}^{-1}$ in the FTIR spectra may be assigned to a vibration of hydroxyl–tin bonds of different organic types of surface hydroxyl groups. A broad peak in the range between 1230 cm^{-1} and 1430 cm^{-1} demonstrates that a small amount of adsorbed water and NO_3^- ions exist in the powder particles. A strong peak centered at $\sim 2355 \text{ cm}^{-1}$ indicates that the tin complex transforms into tin oxide.

It is known that Raman scattering is very sensitive to the microstructure of nanocrystalline materials, and it is also used here to clarify the structure of the SnO_2 nanopowders. As shown in Fig. 7, the first-order Raman spectrum of the as-prepared SnO_2 shows the sharpest and strongest peaks at about $473\text{--}475 \text{ cm}^{-1}$, $631\text{--}633 \text{ cm}^{-1}$ and $773\text{--}775 \text{ cm}^{-1}$, which are in good agreement with those of tetragonal rutile structure of SnO_2 with point group D_{4h} [13], a typical Raman active branch of tetragonal rutile phase of nanocrystalline SnO_2 originated from the non-polar optical phonon E2 (high) mode [14].

The UV–Vis spectrum of nanocrystalline SnO_2 is shown in Fig. 8. The absorption peak shoulder onset

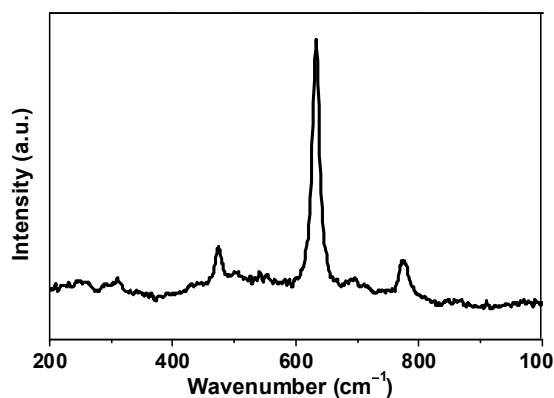


Fig. 7 Raman spectrum of SnO_2 powders.

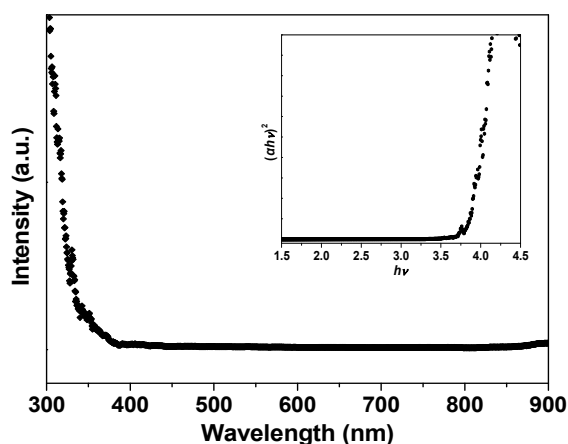


Fig. 8 UV–Vis spectrum of SnO_2 powders.

peaks are located at 340 nm corresponding to the band gap of 3.67 eV. Compared with the other methods (like sol–gel, co-precipitation, etc.), nanocrystalline SnO_2 obtained by this microwave-assisted combustion method has larger band gap energy [13,14]. In general, the hexagonal wurtzite SnO_2 structure has a direct band gap energy (E_g) for the SnO_2 powders and can be determined by extrapolation to the zero absorption coefficient (α) which is calculated from the following equation:

$$\alpha = \frac{2.303A\rho}{IC} \quad (1)$$

where A is the absorbance of the sample; ρ is the density of SnO_2 powders; C is the concentration of the particles; and I is the optical path length. The optical absorption coefficient (α) of a semiconductor is close to the band edge which is estimated from the Tauc's relationship [15] as follows:

$$(\alpha hv)^2 = A(hv - E_g) \quad (2)$$

where α is the absorption coefficient; h is the Planck's constant; ν is the frequency of the incident photon; E_g is the optical direct band gap energy; and A is a constant. The exact value of the band gap is calculated by extrapolating the straight line portion of the $(\alpha hv)^2$ vs. hv curve. Plotting $(\alpha hv)^2$ as a function of photon energy and extrapolating the linear portion of the curve to the photon energy axis (absorption equal to zero) are shown in inset of Fig. 8.

The dependence of particle size of the SnO_2 powders can be determined experimentally from the band gap energy inferred from the optical absorption spectra, which is expressed from an effective mass model [16]. The quantum size effect in the SnO_2 powders can be described from the following equation:

$$E_g^{(\text{nano})} = E_g^{(\text{bulk})} + \frac{h^2}{2D^2} \left(\frac{1}{m_e^* + m_h^*} \right) - 0.248E_{\text{RY}}^* \quad (3)$$

where $E_g^{(\text{nano})}$ is the band gap energy of the synthesized SnO_2 particles; $E_g^{(\text{bulk})}$ is the band gap energy of the bulk material as 3.6 eV; h is the Planck's constant; D is the average crystalline size calculated from PXRD results of SnO_2 powders; the electron and hole effective masses are taken as $m_e^* = 0.299m_0$ and $m_h^* = 0.234m_0$; and the bulk exciton binding energy E_{RY}^* is 130 meV. After simplification of the equation, the band gap energy value is $E_g^{(\text{nano})} = E_g^{(\text{bulk})} + 7.0989D^{-2}$. The optical band gap energy (E_g) was calculated using effective mass equation and from

Tauc's relation as 3.67 eV and 3.71 eV, respectively. Hence the optical band gap energy value appears slightly lower than the calculated band gap energy value (effective mass model) due to a tight-binding model used in the experimental data (optical absorption spectra).

4 Conclusions

Nanocrystalline SnO₂ has been successfully synthesized by a microwave-assisted combustion method using glycine as fuel. PXRD, FTIR and Raman spectra confirm the formation of a tetragonal rutile phase. The crystal structural parameters are in good agreement with the literature values. Besides, there is no peak other than SnO₂ in the synthesized powders. FTIR and Raman spectra confirm the compound formation. SEM micrographs show the uniform particles present in the powders. EDX analyses show that the stoichiometric formation of SnO₂ nanopowders. From absorption spectrum, the band gap energy of the material is estimated as 3.67 eV which is comparable with the bulk value.

Open Access: This article is distributed under the terms of the Creative Commons Attribution License which permits any use, distribution, and reproduction in any medium, provided the original author(s) and the source are credited.

References

- [1] Chen D, Gao L. Facile synthesis of single-crystal tin oxide nanorods with tunable dimensions via hydrothermal process. *Chem Phys Lett* 2004, **398**: 201–206.
- [2] Michel E, Stuerger D, Chaumont D. Microwave flash synthesis of tin dioxide sols from tin chloride aqueous solutions. *J Mater Sci Lett* 2001, **20**: 1593–1595.
- [3] Jiang L, Sun G, Zhou Z, *et al.* Size-controllable synthesis of monodispersed SnO₂ nanoparticles and application in electrocatalysts. *J Phys Chem B* 2005, **109**: 8774–8778.
- [4] Yang H, Hu Y, Tang A, *et al.* Synthesis of tin oxide nanoparticles by mechanochemical reaction. *J Alloys Compd* 2004, **363**: 276–279.
- [5] Pan ZW, Dai ZR, Wang ZL. Nanobelts of semiconducting oxides. *Science* 2001, **291**: 1947–1949.
- [6] Baik NS, Sakai G, Miura N, *et al.* Preparation of stabilized nanosized tin oxide particles by hydrothermal treatment. *J Am Ceram Soc* 2000, **83**: 2983–2987.
- [7] Song KC, Kang Y. Preparation of high surface area tin oxide powders by a homogeneous precipitation method. *Mater Lett* 2000, **42**: 283–289.
- [8] Zhu J-J, Zhu J-M, Liao X-H, *et al.* Rapid synthesis of nanocrystalline SnO₂ powders by microwave heating method. *Mater Lett* 2002, **53**: 12–19.
- [9] Wu D-S, Han C-Y, Wang S-Y, *et al.* Microwave-assisted solution synthesis of SnO nanocrystallites. *Mater Lett* 2002, **53**: 155–159.
- [10] Pires FI, Joanni E, Savu R, *et al.* Microwave-assisted hydrothermal synthesis of nanocrystalline SnO powders. *Mater Lett* 2008, **62**: 239–242.
- [11] Krishna M, Komarneni S. Conventional- vs microwave-hydrothermal synthesis of tin oxide, SnO₂ nanoparticles. *Ceram Int* 2009, **35**: 3375–3379.
- [12] Nehru LC, Swaminathan V, Sanjeeviraja C. Rapid synthesis of nanocrystalline ZnO by a microwave-assisted combustion method. *Powder Technol* 2012, **226**: 29–33.
- [13] Ristić M, Ivanda M, Popović S, *et al.* Dependence of nanocrystalline SnO₂ particle size on synthesis route. *J Non-Cryst Solids* 2002, **303**: 270–280.
- [14] Wu J-J, Liu S-C. Catalyst-free growth and characterization of ZnO nanorods. *J Phys Chem B* 2002, **106**: 9546–9551.
- [15] Tauc J. *Amorphous and Liquid Semiconductor*. New York: Plenum Press, 1974.
- [16] Brus LE. Structure and electronic states of quantum semiconductor crystallites. *Nanostruct Mater* 1992, **1**: 71–75.